Biomaterials Science

Impact of Surface Chemistry and Topography on the Function of Antigen Presenting Cells

Journal:	*Biomaterials Science*
Manuscript ID:	BM-REV-10-2014-000375.R1
Article Type:	Review Article
Date Submitted by the Author:	12-Dec-2014
Complete List of Authors:	Rostam, Hassan; University of Nottingham, Singh, Sonali; University of Nottingham, Vrana, Nihal; Protip SAS, Alexander, Morgan; University of Nottingham, Pharmacy Ghaemmaghami, Amir; University of Nottingham, Immunoloy

Biomaterials Science

RSCPublishing

ARTICLE

Cite this: DOI: 10.1039/x0xx00000x

Impact of Surface Chemistry and Topography on the Function of Antigen Presenting Cells

H.M. Rostam [a], S. Singh [a], N. E. Vrana, [b, c] M. R. Alexander [d] and A.M. Ghaemmaghami*[a]

Received 00th January 2012,
Accepted 00th January 2012

DOI: 10.1039/x0xx00000x

www.rsc.org/

Antigen presenting cells (APCs) such as macrophages and dendritic cells (DCs) play a crucial role in orchestrating immune responses against foreign materials. The activation status of APCs can determine the outcome of an immune response following implantation of synthetic materials, towards either healing or inflammation. A large range of biomaterials are used in the fabrication of implantable devices and drug delivery systems. These materials will be in close contact with APCs and characteristics such as surface chemistry and topography may have a critical role in initiating pro- or anti-inflammatory immune responses. Controlling biomaterial surface attributes provides a powerful tool for modulating the phenotype and function of immune cells with the aim of reducing detrimental pro-inflammatory responses and promoting beneficial healing responses. In this article, we review recent literature on how biomaterial surface topography and chemistry can modulate APC populations towards distinct pro- or anti-inflammatory phenotypes with specific examples of how these properties can be used to control host response *in vivo*. Topographical and/or chemical design of biomaterial surfaces with respect to the APC responses can pave the way for a new generation of 'cell instructive' materials with immunomodulatory properties with a wide range of clinical applications.

Introduction

Exposure of implantable biomaterials to blood can initiate acute innate immune responses through activation of complement and coagulation cascades as well as innate immune cells such as monocytes and polymorphonuclear cells[1]. Preclinical biocompatibility studies ensure that such acute responses can be avoided. However, implants can still induce subtle inflammatory responses that in the long term can have detrimental effects on the function of the implant (e.g. loosening of metal implants) and cause damage to the surrounding tissues. Antigen presenting cells (APCs), particularly macrophages [2] and dendritic cells (DCs) [3], play a central role in orchestrating immune responses to foreign substances including biomaterials [4]. Contact with implanted materials may enhance inflammation by provoking macrophages to release cytokines that cause immune responses by other immune cells such as DCs and lymphocytes. Alternatively, some biomaterials can change macrophage phenotype from pro-inflammatory (M1) towards anti-inflammatory and wound healing (M2), thus improving the host response towards biomaterials [4]. In addition, biomaterials may act as adjuvants in provoking adaptive immune responses particularly by modulating DC responses against implants [5].

*Corresponding author
[a] Immunology and Tissue Modelling Group, School of Life Science, University of Nottingham, Queen's Medical Centre, Nottingham, NG7 2UH, UK.
E-mail: amg@nottingham.ac.uk
[b] Université de Strasbourg, Faculté de Chirurgie Dentaire,
[c] Protip SAS, 8 Place de l'Hopital, 67000, Strasbourg, France
[d] Interface and Surface Analysis Centre, School of Pharmacy, University of Nottingham.

Macrophages have a sensitive and rapid response against foreign material including biomaterials that are implanted in different tissues [2]. As time passes, macrophages and their aggregates, known as foreign body giant cells (FBGCs) and multinucleated giant cells, are recruited to the interface between the tissue and the materials [6]. This sequence of events leads to a foreign body reaction (FBR), which is the last stage of the inflammatory response to an implanted material [7]. Following implantation and the initial contact with the host blood, proteins adsorb on the implant surface according to the specific chemical and physical properties of the surface. This in turn induces the adhesion of monocytes and macrophages, which under the influence of soluble mediators such as IL-4 and IL-13 released by mast cells and later by T helper 2 (T_H2) cells, can fuse to form FBGCs [7]. Macrophages and FBGCs are the primary mediators of FBR, inducing the infiltration and stimulation of immune cells (e.g. lymphocytes) and stromal cells (e.g. fibroblasts) and fibrinogenesis at the implant site **(Figure 1)**. At the end of the FBR the implant can be encapsulated by a fibrous capsule and cut off from the host. This not only creates mechanical and functional problems, but for implanted devices, such as electrodes, can mean the end of their functional life-time.

Although macrophages and FBGCs can cause chronic inflammation and osteolytic activity [8], they also play an important role in regeneration and healing processes via extracellular matrix (ECM) modulation and phagocytosis (ingestion) of microbes, dead cells, and debris as well as promoting vascularisation [2]. Macrophages mediate biodegradation of bioresorbable material and control the differentiation, proliferation, and recruitment of other tissue cells such as osteoblasts, fibroblasts, keratinocytes, and endothelial cells

during the healing process [2]. Various methods have been examined to modulate the interaction between biomaterials surface and macrophages to reduce inflammatory reactions [9, 10]. In this context, it is interesting to note that different surface topographies have been shown to be able to induce specific cellular response in other cell types such as mesenchymal stromal cells [11]. There are many examples of implantable biomaterials used in intraocular lenses [12], coronary stents [13], degradable sutures [14], catheters [15], vascular grafts [16], prosthetic joints [17], cochlea [18] and pace maker replacements [19] as well as in neuronal regeneration [20]. Also many biodegradable biomaterials have been developed for tissue engineering applications [21]. Most of the biomaterials which are widely used clinically have been selected due to their "bio-inertness", i.e. they are known to induce a lesser degree of immune response. But for the new generation of biomaterials where the remodelling is a crucial component, control of the immune response rather than its dampening is more appropriate. It is well-known that the topography and chemistry of these materials has a significant influence on cellular responses [11], but this relationship is complex and still not fully understood, especially for APCs.

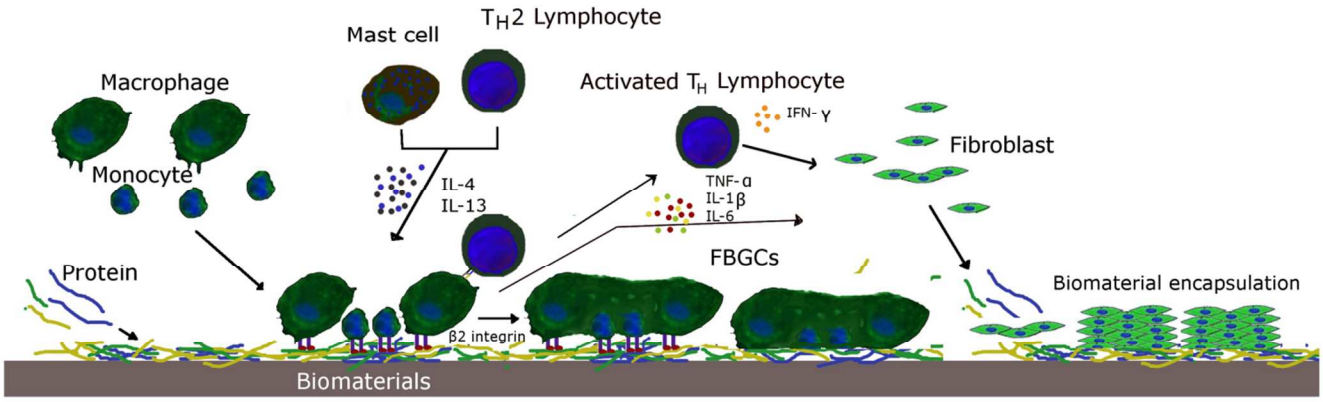

Figure 1: Different types of protein adhere to biomaterials; β2 integrin from cells can mediate cell adherence at the biomaterial surface. IL-4 and IL-13 from mast cell and T_H2 cell stimulate macrophage aggregation and FBGC formation, which secrete primary mediators for immune cells and fibroblasts, causing fibrogenesis and encapsulation of the implanted biomaterial.

The aim of this review is to survey the current observations of how different surface topographies and chemistries could influence cell behaviour, particularly in the context of innate immune responses that are initiated by APCs such as macrophages and DCs. Better understanding of cell-material interactions will allow the development of new strategies for modification of implant surfaces to modulate immune responses towards anti-inflammatory and healing phenotypes.

Antigen Presenting Cells

The adaptive immune response depends on activation signals from APCs [22], which include monocytes, macrophages, DCs, and B cells [23] **(Figure 2).** APCs are sentinels of the immune system that can detect and capture foreign antigens in the periphery. APCs process and present these antigens to T cells in the context of major histocompatibility complex (MHC) molecules [24]. T cell activation by APCs, which typically takes place in the lymph nodes, requires at least two signals: the first signal is delivered by MHC-antigen peptide complex that interacts with T cell receptors, and the second signal is provided by co-stimulatory molecules such as CD80 and CD86 that interact with CD28 on T cell surface. Depending upon the APC's cytokine profile and maturation status, T cells may differentiate to different subsets with distinct functions [25].

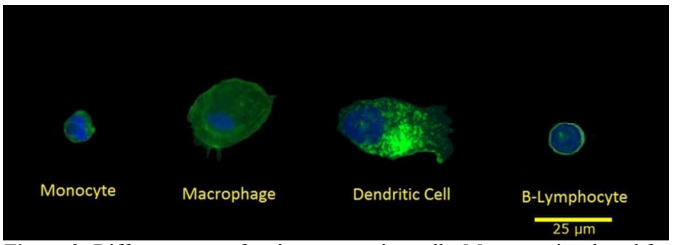

Figure 2: Different types of antigen presenting cells. Monocyte incubated for 2hrs, naïve macrophage (human monocyte treated with GM-CSF for 6 days), dendritic cell (human monocyte treated with IL-4 /GM-CSF for 6 days), B-Lymphocyte. F-actin and cell nuclei immunostaining were performed by Phalloidin Alexa Fluor 488 (green) and DAPI (blue) respectively. Scale bar = 25 µm.

The mononuclear phagocyte system includes a subgroup of leukocytes that originate from myeloid progenitor cells in the bone marrow [26]. Monocytes derived from these progenitors circulate through blood vessels and migrate into tissues in response to pro-inflammatory cytokines, growth factors, or microbial products [27]. Once in tissues, monocytes differentiate into DCs or macrophages [27]. Monocytes as APCs are able to uptake antigen in bone morrow or in the blood vessels [28], but compared to macrophages and particularly DCs they have lower capability of antigen presentation and phagocytic activity [29].

A number of different macrophage phenotypes with distinct functional properties have been identified with a spectrum of activities. The two best studied macrophage phenotypes are M1 or classically activated macrophages and M2 or alternatively activated macrophages. M1 macrophages have pro-inflammatory and anti-tumour activities, while M2 macrophages have anti-inflammatory and pro-wound healing activities [30] **(Figure 3)**. Interferon gamma (IFN-γ) (produced by T helper 1 (T_H1) cells and $CD8^+$ T cells (adaptive immunity) or natural killer (NK) cells (innate immunity)) in the presence of microbial products such as lipopolysaccharide (LPS) induces differentiation of M1 macrophages. On the other hand, interlukin-4 (IL-4) and/or IL-13, which mainly originate from T_H2 cells (adaptive immunity) [31] or from polymorphonuclear cells such as mast cells [32](innate immunity), induce differentiation of M2 macrophages [33]. However, the classification of M2 macrophages is made more complex by the fact that different studies have used the term "M2 macrophage" for macrophages activated with a diverse range of agents: e.g. immune complexes, apoptotic cells, prostaglandins, glucocorticoids, macrophage G-protein coupled

receptor (GPCR) and IL-10 [34]. There has been an effort to acknowledge the differences between these disparate M2 macrophages types by subdividing them into M2a, M2b, and M2c macrophages or defining a third category of "regulatory macrophages" [35]. A recent review by a consortium of macrophage biologists calls for standardisation of macrophage activation protocols and nomenclature, proposing a revised system of nomenclature that explicitly identifies the activating agent – e.g. M(IFN-γ), M(IL-4), M(IL-10), etc. [35]. However, to avoid confusion, in this review we refer to macrophages with pro or anti-inflammatory functions as M1 or M2 respectively.

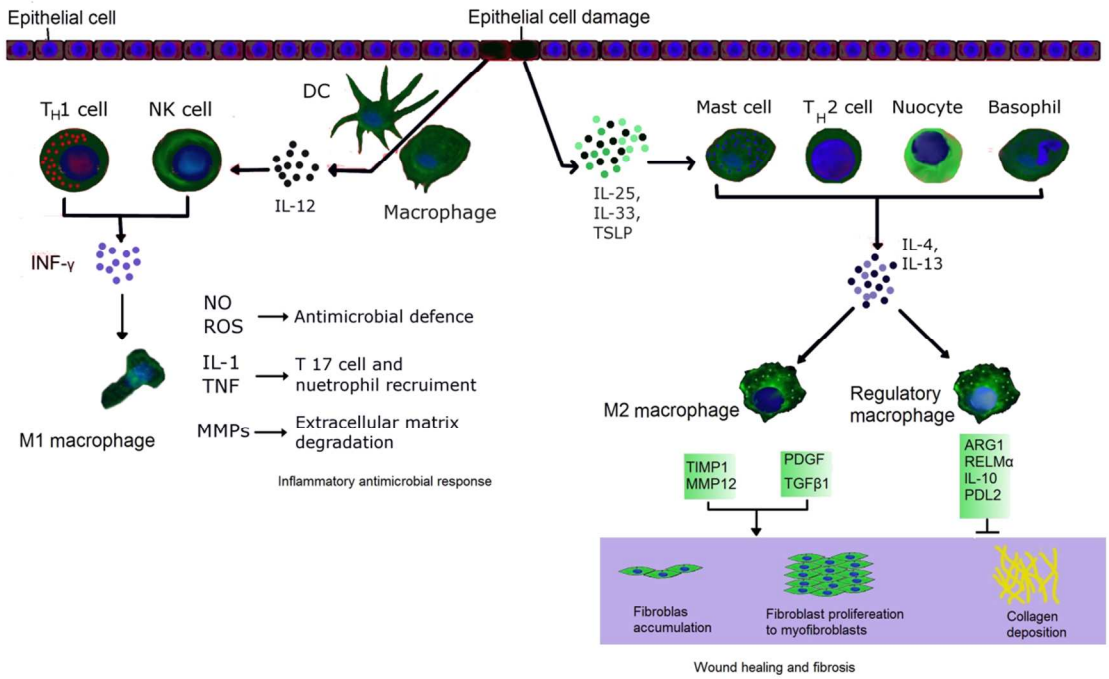

Figure 3: Inflammatory monocytes are recruited to the injured tissue from blood vessels. Under the effect of interferon-γ (IFN-γ) from natural killer (NK) and T_H1 cells, monocytes differentiate into pro-inflammatory M1 macrophages. M1 macrophages express reactive oxygen species (ROS) and nitric oxide (NO), and release tumour necrosis factor (TNF), interleukin-1 (IL-1) and matrix metalloproteinases (MMPs). Thymic stromal lymphopoietin (TSLP), alarmins, IL-25 and IL-33 secretion by damaged tissue induce T_H2 cells, nuocytes, basophils and mast cells to secrete IL-4 and IL-13, which stimulate macrophage polarisation to M2 or regulatory phenotypes. M2 macrophages promote wound healing via secretion of soluble mediators such as platelet-derived growth factor (PDGF), tissue inhibitor of metalloproteinases 1 (TIMP1), MMP12, transforming growth factor-β1 (TGFβ1). Regulatory macrophages express programmed death ligand 2 (PDL2), arginase 1 (ARG1), resistin-like molecule-α (RELMα) and secrete IL-10, which contribute to the wound healing process [36].

Since their discovery by Steinman and Cohn [37], DCs have been shown to be the most potent APCs [38]. DCs are found in different tissues in the body and monitor any signs of threat in the microenvironment, using a host of different pathogen recognition receptors (PRRs) [39]. Typically, DC interaction with foreign antigens leads to the maturation of DCs and their migration to the local lymph nodes where they prime naïve T cells towards distinct functional subsets [40, 41]. In addition, DCs play a vital role in maintaining tolerance towards self-antigens [42].

The importance of the behaviour of distinct APC subsets and the ability to control their polarization have garnered the attention of the researchers in the biomaterials field [43]; however due to the diversity of materials and conditions used, lack of clear definitions and scarcity of mechanistic details, many aspects of how different biomaterials can modulate macrophage and DC function have remained elusive.

Effect of topography on cell function

Non-antigen presenting cells

A variety of strategies have been used to modify the surface topography and chemistry of biomaterials with the aim of altering cellular response and promoting desirable cell phenotypes. Examples of biomaterial topography modifications that have been employed to achieve a range of cellular response changes are presented in **Table 1.** Collectively, these data highlight the significant impact of topographies on behaviour of different cell types.

Some common themes that recur in bio-instructive material design are the ability to control cell migration, attachment, proliferation, and differentiation at an implant site. As each cell type will respond differently to the implant surface, it may be necessary to create multi-purpose surfaces that can influence the behaviour of multiple cell types. The most commonly used surface topographical properties to achieve desired effects are surface roughness and engineered regular surface patterns. Roughness directly affects cell adhesion and spreading through its effects on protein adsorption, whereas regular micro, nanopatterns have important impact on cell size, shape and overall morphology which can indirectly determine cell differentiation and phenotype. This is particularly important for tissues where the cell shape is tightly linked with tissue functions

(heart, bone, cornea etc.) [44]. For instance it has been shown that disordered patterns of square arrays with nano-pits (100 nm depth) placed randomly by up to 50nm on both axes (DSQ50) over a 150μm by 150μm field could significantly promote ontogenesis in mesenchymal stem cells (MSCs) after 21 days in culture. This was in contrast with the effect of highly ordered arrays of square and hexagonal surfaces that showed decreased levels of osteoprogenitor cell density with MSCs retaining a fibroblastic morphology. Intriguingly such DSQ50 topography had a similar efficiency on mesenchymal osteogenesis when compared with osteogenic media (dexamethasone) [45].

Biomaterials Science

RSCPublishing

ARTICLE

Table 1: The effect of surface topography of some biomaterials on the function of non-antigen presenting cells

Material	Surface generation method	Type of surface	Cell type	Effect on cellular response
Poly (lactide-co-glycolide)PLGA membrane copolymer	Patterned on silicon wafers by micromachining	Smooth, grooved (30 µm groove with 45 µm and 175 µm pitch) or rough sandblasted-acid-etched topographies	Osteoblasts and epithelial cells	Microgroove topographies stimulated migration of osteoblasts while rough sandblasted-acid-etched surfaces inhibited epithelial cell migration and proliferation [46]
Commercially pure titanium (SLA)	Acid etched and coarsely blasted			
Polycarbonate	Hot-embossing using silicon master	Plane surface and square offset geometry of nanopit pattern with 120 nm diameter and depth of 100 nm, and with centre spacing of 300 nm ± 50 nm from centre (NSq50)	Human embryonic stem cells	Nanopits stimulated mesodermal differentiation of hESCs with greater degree of efficiency than planar surface with the same chemistry [47]
Silicone elastomer Polydimethyl siloxane (PDMS)	Photolithography	Topographical patterns of 10 µm width, 4 µm depth and 10 µm spacing, arranged in dot-micro-pattern, circular-micro-pattern and linear-micro-pattern	Adult neural stem cells	-All three surface topographies reduced ANSC differentiation in comparison with non-patterned control -CMP and LMP surface topography significantly improved ANSC differentiation to neurons [48]
Silicone elastomer PDMS	Etched in a 20% aqueous solution of potassium hydroxide	Micro-scaled pyramid surfaces, root mean square (RMS) roughness, of ~ 7, 80, and 420 nm and with height of ~ 50, 400, and 1900 nm, respectively	Endothelial cells	Microscaled pyramids eliminated endothelial cell migration and adhesion in comparison with nano-scaled topography [49]
Anodized alumina membrane (AAM)	Oxidation	Nanoporous PDMS (140 nm in diameter), nanoporous anodized alumina membrane (AAM) (140 nm in diameter), and microgrooves patterned PDMS (10 µm, 30 µm, and 50 µm in width, and 2 µm in depth)	Hepatic cells	-Hepatic cell migration speed on nanoporous surfaces was significantly higher than on flat surfaces - Nanoporous AAM and PDMS induced formation of spherical cells. PDMS microgrooves however stimulated the cells to become elongated [50]
Silicone elastomer PDMS	Micro-contact printing technique			
Polyurethane	X-ray lithography	1.4 µm ridge width, 0.4 µm groove, or 4 µm, pitch (ridge width+ groove), with 0.3 µm groove depth	Rabbit coronial fibroblasts	1.4 µm topography reduced myofibroblast in comparison with other topographies and planar surface [51]
Polymethylmeth acrylate (PMMA)	Electron beam lithography followed by nickel die fabrication and then hot embossing	120 nm, diameter;100 nm, depth with space of 300 nm centre–centre with five different array arrangement: square; hexagonal array; square array disordered with 50 nm offset in pit placement; 20 nm, and 150 nm	Stem and progenitor mesenchymal cells	120 nm pits, square array disordered with 50 nm offset in pit placement stimulates osteogenesis from stem and progenitor mesenchymal cell [45]
PMMA	Electron beam lithography	120 nm, diameter;100 nm deep with space of 300 nm centre–centre two different array arrangement, absolute square lattice symmetry, and square array disordered with 50 nm offset in pit placement	Human mesenchymal cells	Absolute square lattice symmetry maintained mesenchymal stem cell phenotype for 8 weeks and kept the cell multipotency for 28 days [52]
Collagen scaffold	Photolithography and chemical etching of Silicon template followed by pouring a Poly(dimethylsiloxane)(PDMS) prepolymer– catalyst mixture onto the silicon wafer and then collagen solution was poured onto a patterned PDMS	Micropatterned collagen films with microchannels of 39 µm groove depth, 8 µm groove width and 3.3 µm ridge width.	Human primary corneal fibroblasts (Keratocytes)	Obtainment of keratocyte alignment with the micropatterns, improved transparency in keratocyte seeded, micropatterned films compared to patterned films [53]
Nanosheet surface structure of titanium alloys	NaOH to form TNSs coated Titanium alloy	With surface roughness (RA) ~48 nm	Rat bone marrow (RBM) cells	NaOH treated TNSs has stimulated RBM to increase osteogenesis, cell adhesion -proliferation, mineralization osteocalcin deposition, and alkaline

				phosphatase activity in comparison with smooth untreated TNS [54]
Silicon scaffolds	Silicon scaffolds etched in hydrofluoric acid (HF) solution in ethanol then oxidised at 800 C° for one hour	With pore diameter of ~36 nm	Human dental pulp stem cells (DPSC)	Stimulated the formation of lateral filopodia protruding from the DPSC cell body[55]
Gallium nitride (GaN) film	-GaN film grown on c-plane sapphire by metalorganic chemical vapor deposition -mechanically polished -Porous substrates were generated by electroless wet chemical etch -GaN nano wire (NW) nitrogen plasma etched	Non treated with RA of ~3.4 nm ,polished ~ 10nm, etched nanoporous ~13 nm and GaN NW surfaces expressed as nano-pillars with diameter of ~ 100nm	Rat pheochromo ytoma (PC12) cells	Roughness has stimulated cell adhesion and differentiation in neurotypic cells [56]

Biomaterials Science

RSCPublishing

ARTICLE

Antigen Presenting Cells
Macrophages

Table 2: The impact of some surface topographies on macrophage function

Material	Surface generation method	Surface topography	Cell polarisation	Secretion	Proliferation	Adhesion
Perfluoropolyether (PFPE) microstructures	Replica molding from silicon masters	Microgrooves with 10 μm width and 5 μm height	27E10+ macrophage (M1 marker) ↑	Pro-inflammatory mediators ↑	No data	No data [57]
		Cylindrical pillars with 20 μm height and diameter	CD163+ macrophage (M2 marker) ↑	Anti-inflammatory mediators ↑	No data	No data [57]
Hydrogel	Electrospinning of nanofibres	2D planar PLGA surface of nanofibrous meshes with or without the bioactive peptide sequences GRGDS or GLF	CD163+ macrophage↑	Pro-inflammatory cytokines ↑	No data	↑ [58]
		3D network of nanofibrous meshes of hydrogel modified PLGA with or without the bioactive peptide sequences GRGDS or GLF	27E10+ macrophage ↑	Pro-angiogenic chemokines ↑	No data	↓[58]
Poly (2-hydroxyethyl methacrylate-co-methacrylic acid) hydrogel scaffolds	Spherical pore network interconnected by channel walls were formed by microsphere templating -Parallel channels formed by polymer fibre templating	Cellular scaffold with pore diameter of 30-40 μm	Mannose receptor (MR) (M2 marker) ↑	Angiogenesis ↑ Fibrotic response↓	No data	No data [59]
Polydioxanone (PDO) scaffold	Electrospinning	Fibre diameter 0.35 μm, and pore radius of 0.6 μm	Arginase 1 (M2 marker) ↓ Nitric oxide synthase (M1 marker) ↑	Angiogenic cytokines VEGF, TGF-b1 and bFGF ↓	No data	No data [60]
		Fibre diameter 2.8 μm, and pore radius 14.73 μm	Arginase 1 (M2 marker) ↑ Nitric oxide synthase (M1 marker) ↓	Angiogenic cytokines VEGF, TGF-β1 and bFGF ↑	No data	No data [60]
Lines of fibronectin	Microcontact printing using PDMS stamps	Micropattern groove with width of 20 μm	arginase-1 ↑	IFN-γ ↓ IL-4and IL-13↑	No data	No data [61]
		Micropattern groove with width of 50 μm Non patterned	Non-significant (NS)	NS	No data	No data [61]
Epoxy	Impressions of commercial sandblasted and acid etched polished titanium topography disks were made in vinyl polysiloxane, then these impressions were filled with epoxy resin	Epoxy impresions surface with average roughness of 4.33 μm	Arginase 1 (NS) Nitric oxide synthase (NS)	-M1 chemokines IFN-γ-induced protein 10 (IP-10)↓ -Monocyte chemotactic protein-1 (MCP-1) ↑ -Macrophage inflammatory protein-1α (MIP-1α) ↑	No data	No data [62]
		Smooth polished epoxy	Arginase 1 (NS) Nitric oxide synthase (NS)	IP-10 ↑, MCP-1 ↓, MIP-1α ↓	No data	No data [62]
Electrospun poly (L-lactic) (PLLA) scaffolds	Electrospinning	Microfibres ~1.5 μm diameter , aligned and random microfibers, aligned nanofibres, and random nanofibers with diameter of ~ 0.5 μm	No data	Nanofibres ↓ pro-inflammatory cytokines and chemokines in comparison with microfibres	No data	↑ Aligned micro and nanofibres in comparison with random micro and nanofibres

						[63]
Polyvinylidene fluoride (PVDF) fluoropolymer	Laser ablation	Dome-like microstructure topographies, 1.8 μm height and about 10 μm diameter with spacing of 30 μm centre-to-centre	↑ CD163 and 27E10 expression in microstructure topographies when compared with nanostructures	↑ Pro-inflammatory cytokines in comparison with nanostructure topographies	No data	No data [64]
	Nano-powdered alumina	Nanostructure with roughness ~100nm and high of 250nm				
Epoxy	Impressions of commercial sandblasted and acid etched, polished , sand blasted and acid-etched titanium topography disks were made in vinyl polysiloxane, then these impressions were filled with epoxy resin	Mechanically polished with Roughness values RA of 0.06 μm	No data	PO and CB stimulated the cells to ↑ IL-1β secretion followed by E and then SLA	No data	PO> CB> E> SLA [65]
		coarse sand blasted , with RA ~ 5 μm,				
		acid-etched, with average RA of 0.58 μm				
		Sandblasted and acid etched surfaces with average RA 4.33 μm				
Epoxy-resin replica surfaces	Impressions of commercial sandblasted and acid etched polished titanium topography disks were made in vinyl polysiloxane, then these impressions were filled with epoxy resin	Sandblasted and acid etched epoxy surface with average roughness of 4.33 μm	No data	-SLA Stimulated macrophage to spherical phenotype -PO changed the macrophage shape from spherical to well spread	No data	NS [66]
		Smooth polished epoxy				
Expanded polytetrafluoroethylene (ePTFE) polymer	Obtained from Biaxially-expanded PTFE filter size 3 μm	ePTFE microgroove with intranodal distances of ~ 4.4	Cell spreading on 4.4μm-ePTFE < flat PTFE film	4.4 μm-ePTFE stimulated the ↑ pro-inflammatory cytokine (IL-1β) secretion when compared with flat PTFE film	No data	4.4 μm-ePTFE ↑ cell adhesion in comparison with flat PTFE film [67]
ePTFE	Obtained from Biaxially-expanded PTFE filter size 3 μm	ePTFE microgroove with intranodal distances of ~ 4.4	After subcutaneously implanting PTFE in mice for 4 weeks Capsule thickness of 4.4 μm-ePTFE ↓ in caparison with flat PTFE film	4.4 μm-ePTFE stimulated IL-1β ↑ IL-6, TNF-α, MCP-1, and macrophage inflammatory protein 1-β ↑ in comparison with flat PTFE film	No data	No data [68]
ZnO	Solution-based hydrothermal growth	Nanorods approximately 50 nm in diameter and about 500 nm height with RA of 31 nm and flat ZnO	Nanorod ZnO reduced Cell viability when compared with flat ZnO	No data	No data	Nanorod ZnO ↓ cell adhesion in comparison with flat ZnO [9]
Tantalum oxide nanodot arrays	Anode aluminium oxide processing	Nanodot arrays; 10 nm and 50 nm diameter and height with dot-to-dot distance of ~20 nm and 60 nm, respectively.	Cell spread 50nm>100nm>200nm	(NS)	No data	50nm nanodot array ↑ cell adhesion in comparison with other nanodot arrays [69]
		Nanodot; 100 nm and 200 nm diameter, height of ~100 and 150 nm, respectively and with dot-to-dot distance of ~110 nm and 190 nm, respectively.				
Carbon nanotubes (CNT) on polycarbonate urethane (PCU) polymer	Glass coated with PCU followed by coating with Cu grids arranged in spacing distance of 30 μm, 60 μm and 100μm. Inter Cu grid spaces	CNT coating on polymer with widths of 30 μm, 60 μm and 100μm	No data	No data	↓	↓ [70]

	were coated with CNT solution. Cu grid were removed to form CNT array on PCU					

Biomaterials Science RSCPublishing

ARTICLE

The topography of biomaterials has a critical effect on macrophage activity. Studies describing the effect of biomaterial topography on macrophages are tabulated in **Table 2**.

Microstructures have been shown to have significant effects on macrophage phenotype. Recently, 20 µm wide lines of fibronectin but not 50 µm wide lines (printed on a PDMS surface) were shown to induce elongation of mouse bone marrow–derived macrophages (BMDMs) and promote their differentiation towards M2 phenotype *in vitro* [61]. However, a similar study with human macrophages where human monocytes were seeded on perfluoropolyether microstructures with the same surface chemistry but different topographies for 7 days showed M1 and M2 polarisation in responses to a different set of topographies[57]. It was observed that the surfaces with regular microgrooves of 10 µm width and 5 µm height induced M1 macrophages. In contrast, M2 macrophages were induced by cylindrical pillars (not grooves) with height and diameter of 20 µm and with inter-pillar distance of 70 µm. Smaller pillars with a height and diameter of 3 µm and 6 µm inter-pillar distance resulted in macrophages secreting pro-inflammatory cytokines more than the same size pillars but with 23 µm distance between them [57] **(Figure 4).** In another study, polyvinylidene fluoride (PVDF) with dome-like microstructure topographies, 1.8 µm height and about 10 µm diameter, were shown to significantly promote production of pro-inflammatory cytokines by human macrophages in comparison with randomly nano-textured surface (roughness >100 nm and height average 250 nm) and smooth surface of same chemistry after 7 days of incubation [64]. These observations show the importance of surface feature dimensions for the control of macrophage responses. They also demonstrate that macrophage responses will vary depending upon the species from which the cells are derived, the substrate used for fabrication of microstructures as well as the dimensions of the microstructures.

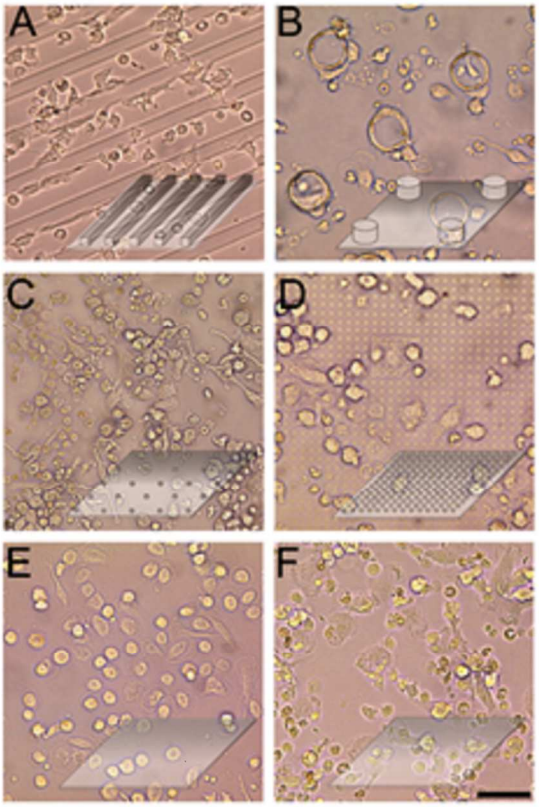

Figure 4: Macrophages on day 7 of culture on different surface topographies. (A–E) PFPE; (F) PVDF. (A) Lines; (B) large posts; (C) more widely separated small posts; (D) more closely packed small posts; (E) smooth PFPE; (F) smooth PVDF. Bar = 30 µm. Figure taken from reference [57].

The effect of substrate depth and porosity on macrophage behaviour is another parameter that has been studied by various researchers. Bartneck *et al* focused on the effect of 3D porous structures vs 2D flat structures on human macrophage phenotypes *in vitro* by using a 3D network of PLGA nanofibrous mesh and 2D planar surfaces both with the same hydrogel surface chemistries. They found that the 2D flat surfaces caused an increase in the expression of CD163+ (an M2 marker) on macrophages. Surprisingly, this was accompanied by secretion of pro-inflammatory cytokines [58], which is considered unusual for anti-inflammatory (i.e. M2) macrophages [71, 72]. In contrast, 3D hydrogel modified PLGA meshes elicited expression of MRP8/14 (27E10 antigen) (an M1 Marker) on macrophages, with a considerable increase in pro-angiogenic chemokine secretion but a decline in pro-inflammatory cytokine secretion [58]. These results suggest that utilisation of a single marker for assessing macrophage phenotype could lead to erroneous conclusions. Further, it indicates that macrophage responses to biomaterial surfaces are complex and could generate mixed functional phenotypes.

Yet in another study, where poly (2-hydroxyethyl methacrylate-co-methacrylic acid) hydrogel scaffolds were used, it was shown that scaffolds with 30-40 µm micropores enhanced human M2 macrophage activation *in vitro* [59]. In addition, human

monocytes/macrophages have been seeded on Polytetrafluoroethylene (PTFE) biomaterial with different surface topography, 4.4 μm intranodal distance 4.4 μm- expanded PTFE (ePTFE), 3.0 μm-ePTFE, 1.2 μm-ePTFE and flat PTFE film. A higher amount of pro-inflammatory cytokine interleukin 1 beta (IL-1β) secretion was found on 4.4 μm-ePTFE surface topography in comparison with flat PTFE film [67]. Furthermore, in a similar study, Bota *et al*, cultured human monocytes/macrophages on the same materials namely ePTFE with different surface topographies [68]. They too observed that 4.4 μm-ePTFE surface stimulates macrophages to secrete 15-fold more IL-1β than np-PTFE surface. On the other hand, 1.2 μm-ePTFE and 3.0 μm-ePTFE surfaces resulted in macrophages secreting an intermediate level of IL-1β. In addition, they found a thinner fibrous capsule by subcutaneous implantation in mice from 4.4 μm-ePTFE surface than flat PTFE film [68].

Micro and nanofibres from different materials are widely used for tissue engineering applications and fibre diameter has been shown to influence immune responses. Garg *et al* cultured mouse bone marrow-derived macrophages (BMDMs) on Polydioxanone (PDO) with fibre diameter of 0.35 μm, 2.2 μm, and 2.8 μm and intra fibre pores with radii of about 1 μm, 11 μm and 15 μm respectively [60]. The study showed a correlation between increase in fibre diameter / pore size and up-regulation of arginase 1 (a M2 marker) and down-regulation of the expression of a M1 marker (nitric oxide synthase). They also found the effect of pore size was more significant than fibre diameter in terms of BMDM polarisation [60]. Fibre diameter and alignment in electrospun poly (L-lactic) (PLLA) scaffolds have also been shown to have a significant effect on secretion of inflammatory cytokines by mouse macrophages (RAW 264.7 cell line) at 24 h and 7 days. Macrophages were cultured on four different types of PLLA fibrous scaffold namely aligned microfibres ~1.5 μm diameter, random microfibres ~1.5 μm diameter, aligned nanofibres ~0.5 μm diameter, and random nanofibres ~0.5 μm diameter. Data suggested that the fibre diameter particularly for nanofibrous PLLA, both aligned and random, significantly increased the secretion of pro-inflammatory cytokines and chemokines [63].
Roughness is another important parameter of implant interface, particularly for metallic implant materials. In particular for bone facing implants increase in roughness generally corresponds to an improved behaviour for osteoblasts and mesenchymal stem cells [73]. Thus, it is necessary to assess the effects of changes in roughness on immune cells. An *in vitro* study has demonstrated the impact of two different surface topographies of epoxy on RAW 264.7 macrophage phenotype, polished (Po) and sandblasted-acid etched (SLA) with replica surfaces of average roughness of 0.06 and 4.33 μm respectively. Rough SLA surface was shown to reduce M1 chemokine IFN-γ-induced protein 10 (IP-10), but increase monocyte chemotactic protein-1 (MCP-1), and macrophage inflammatory protein-1α (MIP-1α) [62]. Moreover, other researchers hypothesised that changes in surface topography could influence NF_KB signalling in macrophages leading to a change in pro-inflammatory cytokines (e.g. IL-1β) secretion. To assess this possibility they used four different epoxy surface topographies from titanium disc; mechanically polished (PO) with Roughness values (R_A) of 0.06 μm, coarse sand blasted (CB) R_A ~ 5 μm, acid etched (AE) R_A 0.58 μm, and sandblasted and acid etched (SLA) R_A 4.33 μm. They found that PO and CB surface have the highest impact on murine macrophages and promoted IL-1β secretion followed by AE and SLA respectively [65]. A study by Salthouse *et al*, on the other hand, examined the effect of surface shape and roughness on macrophages and showed a strong correlation between smooth implanted surfaces without physical acute angles and enhanced tissue compatibility [74]. However, the same study showed that the adhesion of macrophages and giant cells to rough surfaces increased chronic granulomatous reaction [74].

The effect of surface topography on macrophages is significant at the nanoscale too. Surface topography of ZnO nanorods with approximately 50 nm diameter, 500 nm height and roughness value of 31 nm was shown to lead to a significant decline in mice bone marrow-derived macrophage adherence in comparison with ordinary flat ZnO and glass [9]. The function and behaviour of macrophages and foam cells (cells differentiate from macrophages filled with fat that play a crucial role in thermogenesis [75]) can be modulated depending upon nanotopography in the absence of bioactive agents. This was demonstrated by Mohiuddin *et al*, who examined nanodot arrays (10-200 nm) to assess the function and growth of macrophages and foam cells, and found that the area of cell adhesion in macrophages increased with 10-50 nm nanodot arrays by about two folds, but decreased with 100-200 nm nanodot by nearly a quarter in comparison with a flat surface. Similar results were observed with foam cells too [69]. Same effect was observed by seeding murine macrophages on polycarbonate urethane imprinted with carbon nanotubes (30 μm, 60 μm and 100 μm width) when compared with flat polycarbonate urethane surface [70]. They found a decrease in macrophage adhesion and proliferation on aligned regions of carbon nanotubes by about three fold after 24 hours and twice after four days of incubation in comparison with polycarbonate urethane surface.

Thus, it can be concluded that surface attributes such as roughness, porosity, presence and type of micro and nano-structures and presence and scale of fibres have profound effects on macrophage phenotype and function. However, these effects are complex and the combination of features promoting either pro or anti-inflammatory macrophage phenotypes are yet be fully elucidated. Nevertheless, data from various studies indicate that biomaterial-stimulated macrophages do not seem to adopt clear-cut M1 or M2 phenotypes, but rather intermediate phenotypes exhibiting some characteristics associated with each of these activation states. This is not surprising given that macrophages are extremely plastic cells that can assume a wide spectrum of activation states and respond to subtle microenvironmental changes Therefore, when assessing macrophage responses to biomaterials, it is important not to depend upon a single marker or very narrow set of markers to determine macrophage activation, but rather to complement phenotypical analyses with functional analyses that will be relevant to the intended application of the biomaterial.

Dendritic Cells

Compared to macrophages the effect of surface topography on human DC function is less studied. Nevertheless, existing data clearly shows that the surface characteristics of biomaterials could influence DC function. For example Kou *et al.* have investigated this by using different topographies of clinical grade titanium available commercially for dental implants. Investigated topographies in these studies include smooth pre-acid etched treatment (PT), rough sand blasted and acid etched (SLA), and modified SLA (modSLA) which has same roughness of SLA but includes carbonate and hydrocarbonates groups. PT and SLA surfaces stimulated the maturation of DCs as evidenced by expression of higher amounts of CD86 (co-stimulatory molecule and DC maturation marker) and pro-inflammatory cytokines compared to immature DC controls. By contrast, the modSLA surface maintained DCs in a non-inflammatory, immature state, where expression of CD86 was similar to that of immature DC controls [76].

In other experiments, Kou *et al.* used a library of 2,176 different topographies fabricated on a chip [77] to investigate their effect on human DC-like cells. However, they did not observe any reproducible changes in DC-like cells in response to different patterns on the chip [78].

Effect of surface chemistry on cell function

Non-antigen presenting cells

Different aspects of cell adhesion, differentiation, proliferation, and migration can be influenced extensively by the physical and chemical properties of biomaterial surfaces [79].

Table 3 summarises examples of how the function/phenotype of different cell types can be modulated through changes in the surface chemistry where the main set of effects are the chemical groups available on the surface layer and the wettability of the surfaces. Different cell types show different tendencies towards their interaction with the surface wettability and chemical groups, which can be exploited to control their behaviour.

Table 3: The impact of surface chemistry on non-antigen presenting cells

Material	Sample generation method	Surface chemistry	Cell type	Effect on cellular response
Poly(ethylene glycol) (PEG) hydrogel	Photoinitiated mixed-mode thiol-acrylate were used to incorporate peptide sequences into the PEG macromer networks	-PEG gel + enzymatically cleavable RGD (arginine-lysine-aspartic acid) peptides -PEG gel +un-cleavable RGD peptide	Human mesenchymal stem cells (hMSCs)	RGD-releasing gels induced chondrogenesis of encapsulated hMSCs in comparison with persist PEG gel [80]
Poly(ethylene glycol) (PEG) hydrogels	The action of the thiol group on peptides at the ends of a Polyethylene glycol tetra-acrylate, conjugates laminine Ile-Lys-Val-Ala-Val peptide and different concentrations of the synthesized peptide to PEG hydrogels	Poly(ethylene glycol) hydrogels conjugated with short peptide sequence: Ac-Cys-Cys-Arg-Arg-Ile-Lys-Val-Ala-Val-Trp-Leu-Cys	Human neural stem/progenitor cells (hNSCs)	The short peptide stimulated attachment, proliferation of hNSCs, and enhanced the differentiation of them into neurons [81]
Alkanethiolates monolayer on gold	Thiol self-assembly	Functional groups such as CH_3, COOH, OH, NH_2, SH, Br and Phenyl.	Human adipose stem cells (hASCs)	-NH_2 surface was the most and CH_3 surface was the least stimulatory of the growth rate among the surfaces. -Br surface caused adipogenic differentiation of HASCs. -NH_2 promoted osteogenic differentiation, while SH and phenyl surfaces induced chondrogenic differentiation [82].
Silicon (Si)	Plasma polymerisation	Si coated with octadiene (OD) plasma polymer, followed by coating with acrylic acid (AA) plasma polymer and the final coating with diethylene glycol dimethyl ether (DG) plasma polymer gradient layer.	Mouse embryonic stem(ES) cell	Maximal attachment of ES and number of ES colony was higher in AA –plasma- rich end and decreased gradually toward DG-plasma rich end [83]
Glass	Plasma polymerisation	-Uniform samples of hexane with WCA˚ of 10,17,34,42,63,71,80,98 -Linear gradient of Hexane, with WCA˚ escalated from 35 in one end to 90 in other end -Radial gradient, with WCA˚ of about 90 in centre area and decreased gradually to about WCA˚ of 55 in the edge of the gradient	Embryonic rat hippocampal neurons	- By decreasing of hydrophobicity on all samples, the cell adhesion, average length of cell process and cell process number was decreased -Gradients induced the increase of cell density and average process length in comparison with uniform samples with similar wettability [84]
Polystyrene	Oxygen plasma etching	Hydrophilic tissue culture polystyrene (TCP) Hydrophobic (unmodified polystyrene)	Corneal epithelial cells	Hydrophilic TCP surfaces enhanced cell attachment [85]
Gold, chromium, zirconium, titanium, tantalum and niobium	Physical vapour deposition sputter coating of titanium	Gold, chromium, zirconium, titanium, tantalum and niobium	Primary human osteoblasts	All surfaces had a little modulatory effect on cell differentiation, viability, and gene expression [86].
Polystyrene	Super-hydrophobic surfaces achieved using one phase separation methodology Super-hydrophobic surfaces achieved using Argon plasma	Super-hydrophilic Super-hydrophobic	Myoblasts	Super-hydrophilic can influence protein adsorption and myoblast differentiation[87]
Polystyrene	Ultra-violet Ozone (UVO) modification	UV/Ozone treatment treated for 20 s.	Chinese Hamster Ovarian (CHO) cells	The attachment of CHO cell on treated PS with UV/Ozone was significantly higher than no-treated PS after 24 and 48 h of incubation [88]

Silicon wafers	SiOx plasma coating	Range of Hydrophilic (WCA˚~ 26) to hydrophobic (WCA˚ ~98.)	Vascular endothelial cell (EC)	Wettability had opposite effect on cell adhesion/migration of Vascular endothelial cell (EC) when they observed that hydrophilic surfaces enhanced cell adhesion but inhabited cell migration and vice versa [89]
Polymers with graduated amine-hydrocarbon chemistry	Micro-patterns were achieved by hot embossing against a silicon master. Surface chemistry modification was obtained by plasma polymer coating.	Surface chemistry combined with series of microgrooves (width scaled from 5-95µm and with a depth of 3.4 µm) orthogonally	Primary neurons And radial glia	-Mid-range wettability in grooved surfaces (width 5–10 µm) caused axonal alignment. -Radial glia cells were found to prefer extreme hydrophilic and hydrophobic chemistry in groove width of 6-35 µm [90].
Polymer chemical gradients	Micro-patterns were formed by hot embossing against a silicon master. Surface chemistry modification was achieved by plasma polymer coating	Parallel grooves with widths scaled from 5µm to 95µm, each groove combined with WCA˚ varying from 55-95 (Chemistry=amine-hydrocarbon)	NIH 3T3 fibroblasts	-Cells aligned with grooves and coverage increased at WCA˚ 68 –76, groove width 40–60 µm area -Surface wettability influences fibroblast coverage more than groove widths [91]
Silicon (Si)	Ultrafast laser structuring	Gradient dual-scale roughness at micro- and the nano-scale combined with different wettability	NIH 3T3 fibroblasts	Small ratios of roughness enhanced cell adhesion independently of surface chemistry but change of surface wettability by silanization to super-hydrophobic and oxidization to super-hydrophilic for the same degree of roughness affected cell adhesion [92].
PDMS	Oxygen plasma etching of 0.5 mm thick layer of PDMS generated on glass slide then coated with hydrophobic alkylsilane monolayers then every 2 mm wide exposed for ultraviolet ozone (UVO) oxidation, by the decreasing of exposure time a gradient has been made	PDMS gradient with WCA˚ escalated from ~ 10° to 100°	NIH 3T3, mouse embryonic fibroblast	There was a significant correlation between hydrophobicity and cell spreading [93]

Antigen presenting cells

Macrophages

The impact of surface chemistry on macrophage phenotype and function has been investigated by different groups **(Table 4).**

Table 4: The effect of surface chemistry on macrophage function

Biomaterials Science RSCPublishing

ARTICLE

Material	Sample generation method	Surface chemistry	Cell source	Effect on cellular function
Polymer	Polyethylene terephthalate film (Mylar1, PET) is coated with poly(styrene-co-benzyl N,N-dimethyldithiocarbamate) (BDEDTC)	PET coated with BDEDTC (WCA˚ ~70) and polymerised with: -Polyacrylamide (PAAm) WCA˚ ~46±12 -Sodium salt of acrylic acid, (AANa) WCA˚ ~24 -Methyl iodide salt of N-[3-(dimethylamino)propyl] acrylamide, (DMAPAAmMeI) WCA ~31˚	Human monocytes	Polyacrylamide (PAAm) enhanced adherent cells to: Anti-inflammatory cytokine IL-10 ↑ Pro-inflammatory cytokines IL-1β and IL-6 ↓ Cell adherence density ↓ [94]
Modified silicon	Polymer films were prepared by extrusion	Polycarbonate urethane (Bionate® 80A with WCA˚ ~62)	Human monocytes	Hydrophobic PDMS stimulated spreading of adherent macrophage ↓ By adding IL-4, mannose receptor (MR) expression ↑ in comparison Bionate® 80A [95].
	Silastic_ BioMedical Grade ETR Elastomer Q7-4765	PDMS film with Advancing Contact Angle of 120 °		
Polyethylene terephthalate (PET)	Photograft copolymerization	PET coated with: -Poly(benzyl *N,N*-diethyldithiocarbamateco-styrene) (BDEDTC) (hydrophobic) -Polyacrylamide (PAAm) (hydrophilic) -Sodium salt of poly(acrylic acid) (PAANa) (anionic) -Methiodide of poly(dimethylaminopropyl-acrylamide) (DMAPAAmMeI), (cationic)	Human monocytes	-Hydrophilic and Anionic surface ± IL-4 stimulated ↑ Anti-inflammatory cytokine (IL-10) and cell adhesion -Cationic surface caused ↓ IL-10 and cell adhesion [96]
Polyurethane polymer films	Modified Polyurethane with hard segment of 4,4'-methylene bissphenyl diisocyanate(MDI) extended with butanediol(BD) with polytetramethylen oxide soft segment/+PDMS	Polyurethane modified with Fluorocarbon SMEs, Polyethylene oxide (PEO)SMEs, or Poly(dimethylsiloxane)(PDMS) co-soft segment and SMEs	Human monocytes	-Fluorocarbon SMEs and PEO SME did not affect cell adhesion, fusion and apoptosis -Silicon modification ↑ cell adhesion and apoptosis [97]
Poly-DL-lactide-co-glycolide (PLGA) thin film	Coating	-PLGA+ hydroxyapatite (HA) - PLGA + tricalcium phosphate(TCP)	RAW 264.7 murine macrophage cell line	-PLGA surfaces stimulated multinucleated giant cells (MNGCs) formation - PLGA films was degraded by macrophage and MNGCs [98]
Gold nanoparticles	Gold nanoparticles formed by citrate reduction and seed mediated growth	15, 30, 60, and 90 nm gold nanoparticles coated with 0, 0.16, 0.32, 0.48, 0.64, 0.80, 1.12, and 10 PEG/nm^2	J774A.1 murine macrophage cell line	-In serum independent media macrophage uptake of nanoparticle increased with increasing of size of particles and PEG density. -In serum dependent media, there was a decrease of macrophage uptake, amount and types of protein adsorption with the increasing of PEG density [99]
Polyurethane	D-PHI film preparation were formed by combining divinyl oligomer (DVO),methyl methacrylate (MMA) and methacrylic acid (MAA)	-D-PHI coated and non-coated with collagen -Tissue culture polystyrene (TCPS) coated and non-coated with collagen	Human monocyte	-Collagen coated D-PHI and TCPS had more DNA than the uncoated TCPS after 7days -There was more esterase activity for cells on TCPS than D-PHI (±collagen) after 7 days -D-PHI stimulated the decrease of pro-inflammatory cytokines (TNF-α, high mobility group box 1 protein (HMGB1) and IL-1β)and the increase of anti-inflammatory IL-10 secretion over time when compared to TCPS [100]
Arginine-glycine-aspartate (RGD) Vitronectin (VN)	RGD, VN, and Chitosan (CH) dissolved in phosphate-buffered saline containing calcium and magnesium and then adsorbed	- RGD - CH -VN - Carboxylated	Human monocytes	- CH stimulated macrophage adhesion and FBGC formation - Unmodified and Carboxylated Polystyrene (PS) stimulated

CH coated Polystyrene	in to 24-well polystyrene culture plates	-Unmodified PS		macrophage adhesion but inhibited FBGC formation - RGD, CH and VN adsorbed surfaces stimulated (CD147, CD98 , CD206 and CD13) expression [101]

Biomaterials Science RSCPublishing

ARTICLE

In vitro, neutrally charged (not cationic or anionic) and hydrophilic polyacrylamide (PAAm) surfaces have been shown to induce minimal pro-inflammatory changes in human macrophages including FBGC formation[94]. In addition, such surfaces cause an increase in the production of the anti-inflammatory cytokine IL-10 and a decrease in the production of pro-inflammatory cytokines IL-1β and IL-6, in adherent macrophages after 10 days of incubation. In a similar study McBane *et al.*, observed that degradable polar hydrophobic ionic polyurethane (D-PHI) surface, affected human monocyte-derived macrophages (MDM) by inducing a decrease in the level of pro-inflammatory cytokines (TNF-α, IL-1β and HMGB1) and increase in anti-inflammatory cytokine, IL-10 in comparison with tissue culture polystyrene [100]. Similarly, in another study by Schutte *et al.*, human monocytes/macrophages were seeded on different surface chemistries: polyurethane, polyethylene, polymethyl, expanded polytetrafluoroethylene, 1-vinyl-2-pyrrolidinone, a hydrogel copolymer of 2-hydroxyethyl methacrylate, and polyethylene glycol acrylate in tissue culture polystyrene plates. IL-1β, IL-1rα, IL-6, IL-8, IL-10, TNF-α, MCP-1, MIP-1α, and VEGF were measured at different stages and overall they observed an increase in chemokines, cytokines, and growth factors, as an indicator of monocyte differentiation to macrophages with pro-inflammatory cytokines up-regulated. Surprisingly, production of cytokines was only slightly affected by different surface chemistries [102].

Dadsetan *et al.*, showed a significant effect of hydrophobic (WCA° ~120) PDMS film on protein adsorption and reduction of human macrophage adhesion [95]. In contrast, in similar research by Jones *et al.*, they found that the number of adherent cells on polyacrylamide hydrophilic and neutrally charged surfaces was decreased in comparison with hydrophobic surfaces [94] which was accompanied by a phenotypic switch from pro-inflammatory to anti-inflammatory phenotype where adherent cells showed an increase in anti-inflammatory (i.e., IL-10) and decrease in pro-inflammatory (i.e., IL-1β and IL-6) cytokine production over time. In another study, researchers examined responses of human macrophages and monocytes to two surfaces with terminal methyl group among 14 silane modified glass surfaces. In that study, IL-4 was used to induce formation of FBGC, and GM-CSF was used to enhance adhesion of macrophages. Interestingly they found that, the contact angle and surface energy did not have a significant effect on FBGC formation [103]. In a different set of experiments, Alfarsi *et al.* combined surface chemistry with topography. Different surface chemistries of titanium such as polished (SMO) micro-rough sand blasted, acid etched (SLA) and hydrophilic-modified SLA (modSLA) were shown to differentially regulate macrophage function. For instance, SLA and SMO surfaces elicited up-regulation of 16 pro-inflammatory genes, but modSLA surface down-regulated the expression of 10 genes (TNF, IL-1α and β, CCL1, CCL3, CCL19 and CCL20, CXCL1 and CXCL8, and IL-1 receptor type 1). Collectively, these data indicate that hydrophilic titanium surfaces can modulate pro-inflammatory properties of titanium [104]. While wettability can clearly influence macrophage polarisation in some systems, it is not specific enough a measure to be able to ratinonalise cell response between different classes of materials. For example hydrophilic polyacrylamide [94] and hydrophobic ionic polyurethane [100] can both induce production of anti-inflammatory cytokines by macrophages.

Given the diversity of methods used for generating macrophages and different readouts used for determining their functional phenotype, it is not surprising that some investigators have reported that surface chemistry does not have any significant effect on macrophage polarisation [105],[103]. This highlights the need for more detailed and systematic studies in this area involving multiple material systems.

Dendritic Cells

The effect of biomaterial surface chemistry on DC maturation and inflammatory behaviour is typically studied by culturing immature DCs derived from human peripheral blood monocytes on different biomaterial films. PLGA and chitosan films have been shown to enhance DC maturation (up-regulation of CD80, CD86, CD83, HLA-DQ and CD44) and to stimulate them to secrete pro-inflammatory cytokines [106]. In addition, alginate film has been shown to induce mature DCs to release higher amount of pro-inflammatory cytokines than immature DCs, whereas DCs cultured on hyaluronic acid film exhibited less expression of co-stimulatory molecules and HLA-DR, while agarose film did not affect DC function [106]. In a similar study by Kou *et al.*, the relationship between DC phenotype and biomaterial properties was investigated by assessing the response of DCs derived from human peripheral blood monocytes to 12 different polymethacrylate (pMAs) surface chemistries [107]. In that study, cytokine profile and surface markers were investigated. The investigators found a strong association between DC maturation and carbon- and oxygen-treated pMA surfaces where oxygen treatment maintained immature DC phenotype, whereas carbon-treated surfaces induced strong DC maturation [107]. Furthermore, surface chemistry of biomaterials can influence DCs and differentiate them towards DC1 (pro-inflammatory) or DC2 (anti-inflammatory). Hume *et al.*, showed that magnetic iron oxide nanoparticles (MIONs) stimulated immature DCs and macrophages in mice towards DC1 and M1 phenotypes respectively. Both cell types secreted different T_H1 inducing cytokines such as IL-12 and TNF-α [108]. In contrast, functionalised poly (ethylene glycol) hydrogels with immobilised immunosuppressive factors (TGF-β1 and IL-10) have been shown to decrease murine DC maturation as evidenced by suppression of IL-12 production and expression of major histocompatibility complex-II (MHCII) [109].

As with macrophages, DC function and phenotype can be affected by biomaterials through adsorbed proteins on their surface which interact with DCs via podosomes (cell surface spot-like actin-rich structures that aid cell migration [110]) in a β2 integrin-dependent manner and can affect DC phenotype and Toll-like receptor signalling pathway [111] leading to non-specific inflammatory immune responses [112].

Clinical implications of APC-Biomaterials cross-talk

Immune response related problems are one of the most common reasons that biomaterial based implants fail. The dominant practice to minimise such adverse immune responses is the use of different anti-inflammatory strategies in order to improve the clinical

outcomes. These include i) introduction of anti-inflammatory drugs (both steroidal and non-steroidal) and their controlled release from implant surfaces ii) development of surface coatings that decrease the immune response iii) angiogenic agents to facilitate the integration of the implanted structures [113]. Although, these approaches have provided a fair amount of success and they generally contribute to the improved functionality of implants, in many cases, they are not sufficient for the successful integration and functionality of an implant, particularly in the long term.

The problems related to such approaches mainly stem from the original understanding of biocompatibility where the immune response to a biomaterial was considered detrimental which should be kept at a minimum or suppressed [114]. For example, *in vitro,* poly-ethyleneglycol (PEG) coatings were shown to induce monocyte detachment via a Matrix Metalloproteinase (MMP) dependent manner, which can explain the relatively low level of immune reaction to PEG-coated structures [115]. This can be related to the highly hydrophilic nature of PEG as a general repellent for cell adhesion. However, this approach cannot be applied to biomaterials based structures such as engineered tissues as they need to be remodelled and integrated where the immune response, particularly from monocytic cells like macrophages, play an indispensable part. Thus, the new paradigm in biomaterials research is to communicate with the immune system rather than trying to avoid it. Due to their crucial role in the foreign body response, APCs are the most common target of such approaches. Better understanding of events at the interface between different biomaterials and APCs could pave the way for the rational design of new strategies to harness local immune response to biomaterials to enhance clinical outcomes.

In this context APCs can be targeted to create a favourable cytokine microenvironment (e.g. high IL-10 and TFG-β) to promote healing and implant integration. One possibility to achieve this could be delivering optimally activated APCs to the site of implant via encapsulation. This would be similar to the delivery of insulin producing Langerhans cells used in the treatment of type 1 diabetes [116].

Conclusion

APCs play a pivotal role in response to foreign material and pathogens. Biomaterials are used for manufacturing various implantable medical devices and due to their 'foreign' nature can stimulate the immune system by recruiting neutrophils, macrophages and DCs. Manmade materials can elicit macrophage activation leading to their fusion and adhesion as well as secretion of inflammatory cytokines. Furthermore, biomaterials can also affect DC maturation, and subsequently, stimulate T lymphocyte activation. As a result, inflammation may become a major obstacle in the long-term success of medical devices or implants. Different strategies to modify the surface topography and chemistry of biomaterials have been used to control adverse immune cells-biomaterial interactions or ideally modulate DCs and macrophage phenotype towards anti-inflammatory phenotypes where desirable. Further research in this area may not only achieve optimum surface topography and chemistry to modulate immune cells function to promote healing, tissue regeneration and implant integration but also increase the understanding of how different material properties control immune cell responses.

Acknowledgements:

Authors (SS, NEV and AMG) would like to acknowledge funding from the European Union's Seventh Framework Programme for research, technological development and demonstration under grant agreement no. 602694 (IMMODGEL). HMR is recipient of a PhD scholarship from Kurdistan Regional Government under Human Capacity Development Program in Higher Education (HCDP).

References

1. K. N. Ekdahl, J. D. Lambris, H. Elwing, D. Ricklin, P. H. Nilsson, Y. Teramura, I. A. Nicholls and B. Nilsson, *Adv Drug Deliv Rev*, 2011, **63**, 1042-1050.
2. Z. Xia and J. T. Triffitt, *Biomed Mater*, 2006, **1**, R1-R9.
3. J. E. B. Abensee, *Semin Immunol*, 2008, **20**, 101-108.
4. P. M. Kou and J. E. Babensee, *J Biomed Mater Res A*, 2011, **96A**, 239-260.
5. J. E. Babensee, *Semin Immunol*, 2008, **20**, 101-108.
6. J. M. Anderson, *Curr Opin Hematol*, 2000, **7**, 40-47.
7. J. M. Anderson, A. Rodriguez and D. T. Chang, *Seminars in Immunology*, 2008, **20**, 86-100.
8. E. Solheim, B. Sudmann, G. Bang and E. Sudmann, *Journal of biomedical materials research*, 2000, **49**, 257-263.
9. T. D. Zaveri, N. V. Dolgova, B. H. Chu, J. Lee, J. Wong, T. P. Lele, F. Ren and B. G. Keselowsky, *Biomaterials*, 2010, **31**, 2999-3007.
10. T. D. Zaveri, N. V. Dolgova, B. H. Chu, J. Y. Lee, J. E. Wong, T. P. Lele, F. Ren and B. G. Keselowsky, *Biomaterials*, 2010, **31**, 2999-3007.
11. H. V. Unadkat, M. Hulsman, K. Cornelissen, B. J. Papenburg, R. K. Truckenmuller, A. E. Carpenter, M. Wessling, G. F. Post, M. Uetz, M. J. Reinders, D. Stamatialis, C. A. van Blitterswijk and J. de Boer, *Proc Natl Acad Sci U S A*, 2011, **108**, 16565-16570.
12. C. P. McCoy, R. A. Craig, S. M. McGlinchey, L. Carson, D. S. Jones and S. P. Gorman, *Biomaterials*, 2012, **33**, 7952-7958.
13. V. Karagkiozaki, P. G. Karagiannidis, N. Kalfagiannis, P. Kavatzikidou, P. Patsalas, D. Georgiou and S. Logothetidis, *International journal of nanomedicine*, 2012, **7**, 6063-6076.
14. Y. Cao and B. Wang, *International journal of molecular sciences*, 2009, **10**, 1514-1524.
15. R. S. Smith, Z. Zhang, M. Bouchard, J. Li, H. S. Lapp, G. R. Brotske, D. L. Lucchino, D. Weaver, L. A. Roth, A. Coury, J. Biggerstaff, S. Sukavaneshvar, R. Langer and C. Loose, *Science translational medicine*, 2012, **4**, 153ra132.
16. L. Xue and H. P. Greisler, *Journal of vascular surgery*, 2003, **37**, 472-480.
17. K. S. Katti, *Colloids and surfaces. B, Biointerfaces*, 2004, **39**, 133-142.
18. T. Stover and T. Lenarz, *GMS current topics in otorhinolaryngology, head and neck surgery*, 2009, **8**, Doc10.
19. T. Taguchi, S. Maeba and T. Sueda, *Journal of artificial organs : the official journal of the Japanese Society for Artificial Organs*, 2014.
20. P. Roach, T. Parker, N. Gadegaard and M. R. Alexander, *Surf Sci Rep*, 2010, **65**, 145-173.
21. E. S. Place, N. D. Evans and M. M. Stevens, *Nature materials*, 2009, **8**, 457-470.
22. W. Kratky, C. R. E. Sousa, A. Oxenius and R. Sporria, *Proc Natl Acad Sci U S A*, 2011, **108**, 17414-17419.
23. C. M. Wilke, I. Kryczek and W. Zou, *Int Rev Immunol*, 2011, **30**, 120-126.
24. P. Guermonprez, J. Valladeau, L. Zitvogel, C. Thery and S. Amigorena, *Annu Rev Immunol*, 2002, **20**, 621-667.
25. J. Zhu and W. E. Paul, *Cell Res*, 2010, **20**, 4-12.
26. R. v. Furth and Z. A. Cohn, 1968, 434.
27. C. Shi and E. G. Pamer, *Nat Rev Immunol*, 2011, **11**, 762-774.
28. G. J. Randolph, C. Jakubzick and C. Qu, *Current opinion in immunology*, 2008, **20**, 52-60.
29. H. Schmid, R. Sauerbrei, G. Schwarz, E. Weber, H. Kalbacher and C. Driessen, *Biological Chemistry*, 2002, **383**, 1277-1283.
30. F. S. Sutterwala, G. J. Noel, R. Clynes and D. M. Mosser, *J Exp Med*, 1997, **185**, 1977-1985.

31. D. M. Mosser and J. P. Edwards, *Nat Rev Immunol*, 2008, **8**, 958-969.
32. P. Bradding, I. H. Feather, P. H. Howarth, R. Mueller, J. A. Roberts, K. Britten, J. P. Bews, T. C. Hunt, Y. Okayama, C. H. Heusser and et al., *The Journal of experimental medicine*, 1992, **176**, 1381-1386.
33. S. Gordon and F. O. Martinez, *Immunity*, 2010, **32**, 593-604.
34. F. O. Martinez and S. Gordon, *F1000prime reports*, 2014, **6**, 13.
35. P. J. Murray, J. E. Allen, S. K. Biswas, E. A. Fisher, D. W. Gilroy, S. Goerdt, S. Gordon, J. A. Hamilton, L. B. Ivashkiv, T. Lawrence, M. Locati, A. Mantovani, F. O. Martinez, J. L. Mege, D. M. Mosser, G. Natoli, J. P. Saeij, J. L. Schultze, K. A. Shirey, A. Sica, J. Suttles, I. Udalova, J. A. van Ginderachter, S. N. Vogel and T. A. Wynn, *Immunity*, 2014, **41**, 14-20.
36. P. J. Murray and T. A. Wynn, *Nat Rev Immunol*, 2011, **11**, 723-737.
37. R. M. Steinman and Z. A. Cohn, *J Exp Med*, 1973, **137**, 1142-1162.
38. K. Liu and M. C. Nussenzweig, *Eur J Immunol*, 2010, **40**, 2099-2102.
39. R. Medzhitov and C. A. Janeway, Jr., *Science*, 2002, **296**, 298-300.
40. T. Ohteki, *Allergology International* 2007, **56**, 214.
41. J. Banchereau, F. Briere, C. Caux, J. Davoust, S. Lebecque, Y. J. Liu, B. Pulendran and K. Palucka, *Annu Rev Immunol*, 2000, **18**, 767-811.
42. M. G. Roncarolo, M. K. Levings and C. Traversari, *J Exp Med*, 2001, **193**, F5-9.
43. D. Y. Chau, S. V. Brown, M. L. Mather, V. Hutter, N. L. Tint, H. S. Dua, F. R. Rose and A. M. Ghaemmaghami, *Biomedical materials*, 2012, **7**, 045011.
44. C. S. Chen, M. Mrksich, S. Huang, G. M. Whitesides and D. E. Ingber, *Biotechnology Progress*, 1998, **14**, 356-363.
45. M. J. Dalby, N. Gadegaard, R. Tare, A. Andar, M. O. Riehle, P. Herzyk, C. D. W. Wilkinson and R. O. C. Oreffo, *Nature materials*, 2007, **6**, 997-1003.
46. G. R. Owen, J. Jackson, B. Chehroudi, H. Burt and D. M. Brunette, *Biomaterials*, 2005, **26**, 7447-7456.
47. E. Kingham, K. White, N. Gadegaard, M. J. Dalby and R. O. Oreffo, *Small*, 2013.
48. L. Qi, N. Li, R. Huang, Q. Song, L. Wang, Q. Zhang, R. Su, T. Kong, M. Tang and G. Cheng, *Plos One*, 2013, **8**, e59022.
49. G. Le Saux, A. Magenau, T. Bocking, K. Gaus and J. J. Gooding, *Plos One*, 2011, **6**, e21869.
50. K. Y. Mak, L. Li, C. M. Wong, S. M. Ng, C. W. Leung, J. Shi, H. K. Koon, X. Chen, C. S. K. Mak, M. M. Chan and P. W. T. Pong, *Microelectron Eng*, 2013, **111**, 396-403.
51. K. E. Myrna, R. Mendonsa, P. Russell, S. A. Pot, S. J. Liliensiek, J. V. Jester, P. F. Nealey, D. Brown and C. J. Murphy, *Invest Ophth Vis Sci*, 2012, **53**, 811-816.
52. R. J. McMurray, N. Gadegaard, P. M. Tsimbouri, K. V. Burgess, L. E. McNamara, R. Tare, K. Murawski, E. Kingham, R. O. C. Oreffo and M. J. Dalby, *Nature materials*, 2011, **10**, 637-644.
53. C. Kilic, A. Girotti, J. C. Rodriguez-Cabello and V. Hasirci, *Biomaterials Science*, 2014, **2**, 318-329.
54. S. Komasa, T. Kusumoto, Y. Taguchi, H. Nishizaki, T. Sekino, M. Umeda, J. Okazaki and T. Kawazoe, *Journal of Nanomaterials*, 2014, **2014**, 1-11.
55. P. Y. Collart-Dutilleul, I. Panayotov, E. Secret, F. Cunin, C. Gergely, F. Cuisinier and M. Martin, *Nanoscale research letters*, 2014, **9**, 564.
56. L. E. Bain, R. Collazo, S. H. Hsu, N. P. Latham, M. J. Manfra and A. Ivanisevic, *Acta biomaterialia*, 2014, **10**, 2455-2462.
57. M. Bartneck, V. A. Schulte, N. E. Paul, M. Diez, M. C. Lensen and G. Zwadlo-Klarwasser, *Acta biomaterialia*, 2010, **6**, 3864-3872.
58. M. Bartneck, K. H. Heffels, Y. Pan, M. Bovi, G. Zwadlo-Klarwasser and J. Groll, *Biomaterials*, 2012, **33**, 4136-4146.
59. L. R. Madden, D. J. Mortisen, E. M. Sussman, S. K. Dupras, J. A. Fugate, J. L. Cuy, K. D. Hauch, M. A. Laflamme, C. E. Murry and B. D. Ratner, *Proc Natl Acad Sci U S A*, 2010, **107**, 15211-15216.
60. K. Garg, N. A. Pullen, C. A. Oskeritzian, J. J. Ryan and G. L. Bowlin, *Biomaterials*, 2013, **34**, 4439-4451.
61. F. Y. McWhorter, T. T. Wang, P. Nguyen, T. Chung and W. F. Liu, *P Natl Acad Sci USA*, 2013, **110**, 17253-17258.
62. K. A. Barth, J. D. Waterfield and D. M. Brunette, *J Biomed Mater Res A*, 2013, **101**, 2679-2688.
63. E. Saino, M. L. Focarete, C. Gualandi, E. Emanuele, A. I. Cornaglia, M. Imbriani and L. Visai, *Biomacromolecules*, 2011, **12**, 1900-1911.
64. N. E. Paul, C. Skazik, M. Harwardt, M. Bartneck, B. Denecke, D. Klee, J. Salber and G. Zwadlo-Klarwasser, *Biomaterials*, 2008, **29**, 4056-4064.
65. J. D. Waterfield, T. A. Ali, F. Nahid, K. Kusano and D. M. Brunette, *J Biomed Mater Res A*, 2010, **95**, 837-847.
66. S. Ghrebi, D. W. Hamilton, J. Douglas Waterfield and D. M. Brunette, *J Biomed Mater Res A*, 2013, **101**, 2118-2128.
67. A. M. Collie, P. C. Bota, R. E. Johns, R. V. Maier and P. S. Stayton, *J Biomed Mater Res A*, 2011, **96**, 162-169.
68. P. C. Bota, A. M. Collie, P. Puolakkainen, R. B. Vernon, E. H. Sage, B. D. Ratner and P. S. Stayton, *J Biomed Mater Res A*, 2010, **95**, 649-657.
69. M. Mohiuddin, H. A. Pan, Y. C. Hung and G. S. Huang, *Nanoscale research letters*, 2012, **7**, 394.
70. J. Y. Kim, D. Khang, J. E. Lee and T. J. Webster, *J Biomed Mater Res A*, 2009, **88**, 419-426.
71. K. Takeda, T. Kaisho and S. Akira, *Annu Rev Immunol*, 2003, **21**, 335-376.
72. F. O. Martinez, A. Sica, A. Mantovani and M. Locati, *Frontiers in bioscience : a journal and virtual library*, 2008, **13**, 453-461.
73. L. Ponsonnet, K. Reybier, N. Jaffrezic, V. Comte, C. Lagneau, M. Lissac and C. Martelet, *Materials Science and Engineering: C*, 2003, **23**, 551-560.
74. T. N. Salthouse, *Journal of biomedical materials research*, 1984, **18**, 395-401.
75. P. Shashkin, B. Dragulev and K. Ley, *Current pharmaceutical design*, 2005, **11**, 3061-3072.
76. P. M. Kou, Z. Schwartz, B. D. Boyan and J. E. Babensee, *Acta biomaterialia*, 2011, **7**, 1354-1363.
77. M. Baker, *Nat Methods*, 2011, **8**, 900-900.
78. P. M. Kou, 2011
79. W. Zheng, W. Zhang and X. Jiang, *Adv Healthc Mater*, 2013, **2**, 95-108.
80. C. N. Salinas and K. S. Anseth, *Biomaterials*, 2008, **29**, 2370-2377.
81. X. Li, X. Liu, B. Josey, C. J. Chou, Y. Tan, N. Zhang and X. Wen, *Stem cells translational medicine*, 2014, **3**, 662-670.
82. X. Liu, J. He, S. Zhang, X. M. Wang, H. Y. Liu and F. Z. Cui, *J Tissue Eng Regen Med*, 2013, **7**, 112-117.
83. F. J. Harding, L. R. Clements, R. D. Short, H. Thissen and N. H. Voelcker, *Acta biomaterialia*, 2012, **8**, 1739-1748.
84. M. Zelzer, M. R. Alexander and N. A. Russell, *Acta biomaterialia*, 2011, **7**, 4120-4130.
85. M. D. Evans and J. G. Steele, *Journal of biomedical materials research*, 1998, **40**, 621-630.
86. W. Hofstetter, H. Sehr, M. D. Wild, J. Portenier, J. Gobrecht and E. B. Hunziker, *J Biomed Mater Res A*, 2013.
87. M. Cantini, M. Sousa, D. Moratal, J. F. Mano and M. Salmeron-Sanchez, *Biomater Sci-Uk*, 2013, **1**, 202-212.
88. S. A. Mitchell, A. H. C. Poulsson, M. R. Davidson, N. Emmison, A. G. Shard and R. H. Bradley, *Biomaterials*, 2004, **25**, 4079-4086.
89. Y. Shen, G. Wang, X. Huang, Q. Zhang, J. Wu, C. Tang, Q. Yu and X. Liu, *Journal of the Royal Society, Interface / the Royal Society*, 2012, **9**, 313-327.
90. P. Roach, T. Parker, N. Gadegaard and M. R. Alexander, *Biomater Sci-Uk*, 2013, **1**, 83.
91. J. Yang, F. R. A. J. Rose, N. Gadegaard and M. R. Alexander, *Advanced Materials*, 2009, **21**, 300-304.
92. A. Ranella, M. Barberoglou, S. Bakogianni, C. Fotakis and E. Stratakis, *Acta biomaterialia*, 2010, **6**, 2711-2720.
93. G. Mohan and N. D. Gallant, *J Biomed Mater Res A*, 2014.

94. J. A. Jones, D. T. Chang, H. Meyerson, E. Colton, I. K. Kwon, T. Matsuda and J. M. Anderson, *J Biomed Mater Res A*, 2007, **83A**, 585-596.
95. M. Dadsetan, J. A. Jones, A. Hiltner and J. M. Anderson, *J Biomed Mater Res A*, 2004, **71A**, 439-448.
96. W. G. Brodbeck, Y. Nakayama, T. Matsuda, E. Colton, N. P. Ziats and J. M. Anderson, *Cytokine*, 2002, **18**, 311-319.
97. J. A. Jones, M. Dadsetan, T. O. Collier, M. Ebert, K. S. Stokes, R. S. Ward, P. A. Hiltner and J. M. Anderson, *Journal of biomaterials science. Polymer edition*, 2004, **15**, 567-584.
98. Z. Xia, Y. Huang, I. E. Adamopoulos, A. Walpole, J. T. Triffitt and Z. Cui, *J Biomed Mater Res A*, 2006, **79**, 582-590.
99. C. D. Walkey, J. B. Olsen, H. Guo, A. Emili and W. C. Chan, *J Am Chem Soc*, 2012, **134**, 2139-2147.
100. J. E. McBane, L. A. Matheson, S. Sharifpoor, J. P. Santerre and R. S. Labow, *Biomaterials*, 2009, **30**, 5497-5504.
101. A. K. McNally and J. M. Anderson, *J Biomed Mater Res A*, 2014.
102. R. J. Schutte, A. Parisi-Amon and W. M. Reichert, *J Biomed Mater Res A*, 2009, **88A**, 128-139.
103. C. R. Jenney, K. M. DeFife, E. Colton and J. M. Anderson, *Journal of biomedical materials research*, 1998, **41**, 171-184.
104. M. A. Alfarsi, S. M. Hamlet and S. Ivanovski, *J Biomed Mater Res A*, 2013.
105. M. Cejudo-Guillen, M. L. Ramiro-Gutierrez, A. Labrador-Garrido, A. Diaz-Cuenca and D. Pozo, *Acta biomaterialia*, 2012, **8**, 4295-4303.
106. J. Park and J. E. Babensee, *Acta biomaterialia*, 2012, **8**, 3606-3617.
107. P. M. Kou, N. Pallassana, R. Bowden, B. Cunningham, A. Joy, J. Kohn and J. E. Babensee, *Biomaterials*, 2012, **33**, 1699-1713.
108. M. Zhu, X. Tian, X. Song, Y. Li, Y. Tian, Y. Zhao and G. Nie, *Small*, 2012, **8**, 2841-2848.
109. P. S. Hume, J. He, K. Haskins and K. S. Anseth, *Biomaterials*, 2012, **33**, 3615-3625.
110. C. Gawden-Bone, Z. J. Zhou, E. King, A. Prescott, C. Watts and J. Lucocq, *J Cell Sci*, 2010, **123**, 1427-1437.
111. B. S. Antonio S. Sechi, *Biomaterials Associated Infection*, 2013, 151-173.
112. M. Yoshida and J. E. Babensee, *Second Joint Embs-Bmes Conference 2002, Vols 1-3, Conference Proceedings*, 2002, 619-620.
113. J. Morais, F. Papadimitrakopoulos and D. Burgess, *The AAPS Journal*, 2010, **12**, 188-196.
114. D. F. Williams, *Biomaterials*, 2008, **29**, 2941-2953.
115. H. Waldeck, X. Wang, E. Joyce and W. J. Kao, *Biomaterials*, 2012, **33**, 29-37.
116. Z. L. Zhi, B. Liu, P. M. Jones and J. C. Pickup, *Biomacromolecules*, 2010, **11**, 610-616.

